

Simple eigenvalue-self-consistent $\bar{\Delta}GW_0$ Vojtěch Vlček,^{1,2,*} Roi Baer,^{3,†} Eran Rabani,^{4,5,‡} and Daniel Neuhauser^{1,§}¹*Department of Chemistry and Biochemistry, University of California, Los Angeles California 90095, U.S.A.*²*After July 1 2018: Department of Chemistry and Biochemistry, University of California, Santa Barbara California 93106, U.S.A.*³*Fritz Haber Center for Molecular Dynamics, Institute of Chemistry, The Hebrew University of Jerusalem, Jerusalem 91904, Israel*⁴*Department of Chemistry, University of California and Materials Science Division, Lawrence Berkeley National Laboratory, Berkeley, California 94720, USA*⁵*The Raymond and Beverly Sackler Center for Computational Molecular and Materials Science, Tel Aviv University, Tel Aviv, Israel 69978*

We derive a general form of eigenvalue self-consistency for GW_0 in the time domain and use it to obtain a simplified postprocessing eigenvalue self-consistency, which we label $\bar{\Delta}GW_0$. The method costs the same as a one-shot G_0W_0 when the latter gives the full frequency-domain (or time-domain) matrix element of the self-energy. The accuracy of $\bar{\Delta}GW_0$ increases with system size, as demonstrated here by comparison to other GW self-consistency results and to CCSD(T) predictions. When combined with the large-scale stochastic G_0W_0 formulation $\bar{\Delta}GW_0$ is applicable to very large systems, as exemplified by periodic supercells of semiconductors and insulators with 2048 valence electrons. For molecules the error of our eventual partially self-consistent approach starts at about 0.2eV for small molecules and decreases to 0.05eV for large ones, while for the periodic solids studied here the mean-absolute-error is only 0.03eV.

I. INTRODUCTION

The GW approximation¹ to many-body perturbation theory is often used to calculate electron removal or addition energies and related (inverse) photoemission spectra of molecules, nanostructures, and bulk materials.^{2–15} GW is part of a family of methods that describe the probability amplitude of a quasiparticle (QP) to propagate between two space-time points (\mathbf{r}, t) and (\mathbf{r}', t') with a Green's function $G(\mathbf{r}, \mathbf{r}', t, t')$, the poles of which are the QP energies. The Green's function is obtained perturbatively from a reference (non-interacting) Green's function, $G_0(\mathbf{r}, \mathbf{r}', t, t')$, via a Dyson equation (all equations use atomic units):

$$G(\mathbf{r}, \mathbf{r}', t, t') = G_0(\mathbf{r}, \mathbf{r}', t, t') + \iint G_0(\mathbf{r}, \mathbf{r}_1, t, t_1) \times \\ \Sigma(\mathbf{r}_1, \mathbf{r}_2, t_1 - t_2) G(\mathbf{r}_2, \mathbf{r}', t_2, t') d\mathbf{r}_1 dt_1 d\mathbf{r}_2 dt_2, \quad (1)$$

where $\Sigma(\mathbf{r}_1, \mathbf{r}_2, t, t')$ represents the self-energy. The reference Green's function is typically^{16,17} given by the Kohn-Sham¹⁸ (KS) density function theory (DFT).¹⁹ In GW , the self-energy Σ is approximated as:

$$\Sigma(\mathbf{r}, \mathbf{r}', t) = iG(\mathbf{r}, \mathbf{r}', t) W(\mathbf{r}, \mathbf{r}', t^+), \quad (2)$$

where $W(\mathbf{r}, \mathbf{r}', t)$ is the screened Coulomb interaction, usually evaluated within the random phase approximation (RPA).

A solution of the equations above in requires, in principle, a self-consistent procedure since both $\Sigma(\mathbf{r}, \mathbf{r}', t)$ and $W(\mathbf{r}, \mathbf{r}', t^+)$ depend on $G(\mathbf{r}, \mathbf{r}', t)$. In practice, the self-consistency is often abandoned and the most common GW treatment is based on “one-shot” scheme^{16,17}, which we label as G_0W_0 , since the right hand side of Eq. (2) becomes $G_0(\mathbf{r}, \mathbf{r}', t) W_0(\mathbf{r}, \mathbf{r}', t)$, where W_0 is obtained from a random phase approximation that uses the

KS eigenstates. The one-shot approach improves significantly the KS-DFT results, yet it depends on the choice of the reference system and often underestimates the QP gaps (E_g) and the ionization potentials (I).^{8,20–25} A fully self-consistent solution is computationally extremely demanding^{26–35} and in many situations it yields results that are worse than G_0W_0 .^{8,36,37}

To simplify the problem, a static and Hermitian approximation to the self-energy^{20,38} is sometimes used in the so-called QP self-consistent GW (qp GW), which iteratively updates Σ and QP wave-functions (i.e., Dyson orbitals). The qp GW approach is still computationally expensive and cannot be applied for large systems; further it tends to overestimate E_g ^{37–39} and the ionization potentials^{40–42}, due to an overly strong screened Coulomb interaction.^{37,38,41} Alternatively, the W term is kept “frozen” and self-consistency is sought only in the Green's function.^{8,27,29,37,40,43} This method is termed eigenvalue self-consistent GW (ev GW_0) and it was applied successfully to bulk systems^{8,37,44} and to organic molecules,^{25,27,29} with remarkable success. Even though it is cheaper than other self-consistency methods, Σ has to be recalculated in each iteration, making ev GW_0 out of reach for nanoscale systems with thousands of occupied electronic states.

Here a time domain formulation (Sec. II) is used to derive a simplified ev GW_0 formalism, labeled $\bar{\Delta}GW_0$, where the self-consistency is only a postprocessing step. Hence, as long as one has access to the matrix element of the self-energy at all frequencies or all times, then, irrespective of system size, the computational cost of the self-consistency is negligible (i.e., seconds on a single-core machine) so $\bar{\Delta}GW_0$ costs not more than G_0W_0 .

We specifically combine $\bar{\Delta}GW$ with our stochastic G_0W_0 approach, which has a nearly linear scaling^{45,46}

and enables G_0W_0 for extremely large systems^{47,48}. The stochastic G_0W_0 method has automatically the necessary ingredient for $\bar{\Delta}GW_0$, as it produces the matrix element of the self-energy at all times.

The combined method (stochastic G_0W_0 with $\bar{\Delta}GW_0$) is first tested in Sec. III on molecules, and we find that $\bar{\Delta}GW$ becomes more accurate as the system size increases. Next, we perform stochastic G_0W_0 calculations for periodic semiconductors and insulators using large supercells with 2048 valence electrons. For solids $\bar{\Delta}GW_0$ gives E_g in excellent agreement with experiment and a mean absolute error of 0.03 eV.

In all cases the self-consistency is reached in very few iterations without any additional cost on top of the G_0W_0 step.

II. THEORY

A. Green's function self-consistency in the time domain

The QP energy of the i^{th} state $\varepsilon^{QP}(i)$ is calculated using the usual form of the perturbative GW approximation in which the Kohn-Sham eigenvalues (ε^0) are corrected by the QP shift (Δ) using a fixed point equation:

$$\varepsilon^{QP}(i) = \varepsilon^0(i) + \Delta(i), \quad (3)$$

where

$$\Delta(i) = \tilde{\Sigma}_i[\omega = \varepsilon^{QP}(i)] - \langle \phi_i | v_{xc} | \phi_i \rangle. \quad (4)$$

Here, v_{xc} is the Kohn-Sham exchange-correlation potential for the DFT density, $\tilde{\Sigma}_i[\omega]$ is the Fourier transform of the matrix-element of $\hat{\Sigma}(t)$

$$\tilde{\Sigma}_i[\omega] = \int \langle \phi_i | \hat{\Sigma}(t) | \phi_i \rangle e^{i\omega t} dt, \quad (5)$$

and $\hat{\Sigma}(t)$ is given by Eq. (2).

Starting from a KS DFT reference point, the initial self-energy is constructed from the KS propagator

$$iG_0(\mathbf{r}, \mathbf{r}', t) = \text{Tr} \left\{ |\mathbf{r}\rangle \langle \mathbf{r}'| e^{-i\hat{h}^0 t} \left[\theta(t) \theta_\beta(\hat{h}^0 - \mu) - \theta(-t) \theta_\beta(\mu - \hat{h}^0) \right] \right\}, \quad (6)$$

where Tr denotes a trace over all KS states, μ is the chemical potential, θ is the Heaviside step function that guarantees forward and backward time propagation for particles and holes, respectively, and \hat{h}^0 is the KS Hamiltonian

$$\hat{h}^0 = -\frac{1}{2}\nabla^2 + v_{\text{ext}} + v_{\text{H}} + v_{\text{xc}}, \quad (7)$$

where we introduced the kinetic energy and the external and Hartree potentials. In the rest of the paper

we employ real time-dependent Hartree propagation to calculate the screened Coulomb interaction^{45,46}; this is equivalent to using the RPA approximation for W_0 .

In the time-domain, the self-energy matrix element for the i^{th} state is

$$\langle \phi_i | \hat{\Sigma}_0(t) | \phi_i \rangle = i \iint \phi_i(\mathbf{r}) G_0(\mathbf{r}, \mathbf{r}', t) W_0(\mathbf{r}, \mathbf{r}', t^+) \phi_i(\mathbf{r}') d\mathbf{r} d\mathbf{r}'. \quad (8)$$

Finally, after Fourier transformation combined with time-ordering^{45,46} the ‘‘one-shot’’ QP energy is calculated through Eq. (4).

In the $\text{ev}GW_0$ procedure, the Green's function is reconstructed in each iteration, employing the QP energies from the previous iteration. In the time domain this corresponds to writing the propagator as

$$iG(\mathbf{r}, \mathbf{r}', t) = \text{Tr} \left\{ |\mathbf{r}\rangle \langle \mathbf{r}'| e^{-i(\hat{h}^0 + \hat{\Delta})t} \left[\theta(t) \theta_\beta(\hat{h}^0 - \mu) - \theta(-t) \theta_\beta(\mu - \hat{h}^0) \right] \right\}, \quad (9)$$

where $\hat{\Delta}$ contains all the many-body contributions.

As common in $\text{ev}GW_0$ self-consistency^{37,40,43}, the fact that the true self-energy operator is non-Hermitian and non-diagonal is disregarded and, for the purposes of Eq. (9), it is expressed in the KS basis as

$$\hat{\Delta} \simeq \sum_i |\phi_i\rangle \text{Re}\Delta(i) \langle \phi_i|. \quad (10)$$

Hence, all the KS energies in the exponent in Eq. (9) are shifted to the QP energies obtained from Eq. (3). Eq. (10) is basically the fundamental equation of $\text{ev}GW_0$.

We now note that the operator $\hat{\Delta}$ in Eq. (9) is by construction diagonal in the KS basis set and we thus express it as a function of the KS Hamiltonian $\bar{\Delta}(\hat{h}^0)$ that interpolates all QP shifts. The Green's function is therefore:

$$iG(\mathbf{r}, \mathbf{r}', t) = \text{Tr} \left\{ |\mathbf{r}\rangle \langle \mathbf{r}'| e^{-i[\hat{h}^0 + \bar{\Delta}(\hat{h}^0)]t} \left[\theta(t) \theta_\beta(\hat{h}^0 - \mu) - \theta(-t) \theta_\beta(\mu - \hat{h}^0) \right] \right\}. \quad (11)$$

This simple expression allows for a further approximation described below that significantly reduces the computational cost associated with self-consistent treatment.

B. Efficient and inexpensive implementation

In many cases $\bar{\Delta}$ is well described by a low degree polynomial with discontinuity at the band gap energies, $\varepsilon(H)$ and $\varepsilon(L)$, corresponding to the highest occupied (H) and lowest unoccupied (L) states, respectively. The zeroth

order term in this polynomial corresponds to a scissors operator^{49,50} which shifts the occupied and unoccupied states down and up in energy, respectively

$$\text{Re}\bar{\Delta}[\varepsilon^0(i)] \approx \begin{cases} \Delta(H) & \varepsilon^0(i) \leq \varepsilon^0(H) \\ \Delta(L) & \varepsilon^0(i) \geq \varepsilon^0(L) \end{cases}. \quad (12)$$

We call this approximation $\bar{\Delta}GW_0$ and use it in Sec. III for molecules and periodic systems.

Combining Eqs. (12) and (11) leads to a modified Green's function which acquires an additional phase shift that is different for positive and negative times. Therefore, in the time domain we can define:

$$\bar{\Delta}(t) \equiv \begin{cases} \Delta(H) & t < 0 \\ \Delta(L) & t > 0 \end{cases}. \quad (13)$$

In each iteration, the updated self-energy matrix element is then calculated as

$$\langle \phi_i | \hat{\Sigma}(t) | \phi_i \rangle = e^{-i\bar{\Delta}(t)t} \langle \phi_i | \hat{\Sigma}_0(t) | \phi_i \rangle. \quad (14)$$

Next, the self-energy matrix element is transformed to the frequency domain and used in Eq. (3) to calculate a new estimate of the QP energy. The new QP energy is used iteratively to update Eqs. (12) and (13). The full cycle is illustrated in Fig. 1.

Note that this form of self-consistency is trivial and is a postprocessing step with *no additional cost*, unlike previous uses^{49,50} of the scissors-operator in GW which require repeated evaluations of the self-energy. Further, the $\bar{\Delta}GW_0$ approach is applicable to any implementation which yields $\Sigma(\omega)$. It is naturally suited for the stochastic G_0W_0 method^{45,46} which provides the self-energy on the full-time domain and therefore on a wide range of frequencies (spanning several hundred eV).

III. RESULTS AND DISCUSSION

A. Molecules

We first test our approach on ionization potentials I (taken as $-\varepsilon_H$) for a set of small molecules listed in Table. I. A ground state DFT calculation is performed using a Fourier real-space grid, ensuring (using the Martyna-Tuckerman approach)⁵¹ that the potentials are not periodic. The exchange-correlation interaction is described by local density approximation (LDA)⁵² with Troullier-Martins pseudopotentials⁵³; the DFT eigenvalues are converged up to <10 meV with respect to the spacings of the real space grids (given in Table I).

The systems listed in the table are ordered according to the number of valence electrons; N_2 and hexacene are the smallest and the largest molecules studied here. In all cases, the stochastic G_0W_0 approach^{45,46} was used to calculate the self-energy. We compare our calculations with reference values taken from experiment and from

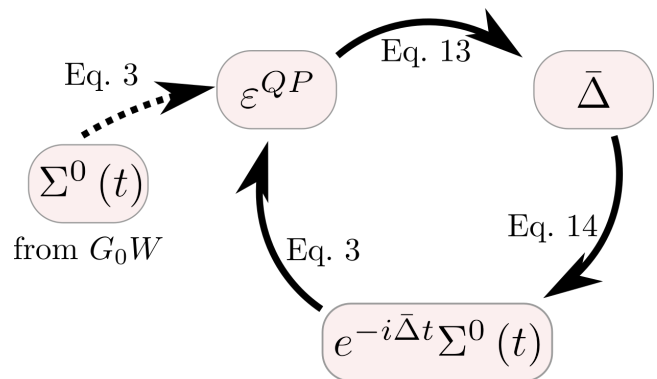


Figure 1. Illustration of the self-consistency cycle (full arrows). In the first step G_0W_0 is used to calculate the self-energy $\Sigma^0(t)$ and the corresponding QP energies ε^{QP} for the HOMO and LUMO states (dashed arrow). The shift of occupied and unoccupied states ($\bar{\Delta}$) is calculated from the QP HOMO and LUMO energies through Eq. (12). The updated time-dependent self-energy $\Sigma(t) = e^{-i\bar{\Delta}t}\Sigma^0(t)$ is obtained via Eq. (13), which leads to new QP HOMO/LUMO energies. The cycle is repeated a few times until reaching self-consistency.

CCSD(T). The geometries of the acene molecules are taken from the GW and CCSD(T) benchmark in Ref. 54.

Compared to the LDA eigenvalues, one-shot G_0W predictions for the ionization potentials are much closer to the CCSD(T) values with a mean absolute error of 0.29 eV. In all cases, the value of I is underestimated, in agreement with previous benchmark studies^{46,54,55}. As the system size increases the difference between the G_0W and CCSD(T) values decreases so that the one-shot correction is an increasingly better approximation.

The simplified eigenvalue self-consistency converges in 3-4 iterations after the initial G_0W calculation; the initial and final self-energy curves are illustrated for hexacene in Fig. 2. Since our self-consistency procedure is merely a postprocessing step, its computational cost is negligible (less than a second on single core machine).

We first compare our $\bar{\Delta}GW$ results with previous eigenvalue and quasiparticle self-consistent GW treatments (ev GW and qp GW , respectively). All methods consistently increase ionization potentials above the one-shot values. The $\bar{\Delta}GW_0$ estimates are higher than ev GW , but appear to be closer to qp GW . As there are very few published qp GW results for molecules, it is not possible to assess whether this is a general trend for molecules.

For all the studied molecules our method yields results in good agreement with CCSD(T). The improvement is only modest for the smallest molecules, since the QP shift strongly depends on ε^0 , i.e., it is not constant for all occupied (or unoccupied) states and the assumption of Eq. (12) is not fulfilled. For instance, for N_2 G_0W_0 shifts the lowest valence state by -7.34 ± 0.06 eV, but the HOMO energy is decreased by -4.63 ± 0.05 eV. In contrast, the shifts are closer for hexacene: -2.73 ± 0.08

system	h (a_0)	I (eV)						
		LDA	G_0W_0	$\bar{\Delta}GW_0$	ev GW_0	qp GW	CCSD(T)	Exp.
nitrogen	0.35	10.44	15.08 (0.05)	15.93 (0.05)	15.32 ^a	16.01 ^a	15.57 ^b	15.58
ethylene	0.35	6.92	10.50 (0.04)	10.87 (0.04)	10.24 ^a	10.63 ^a	10.67 ^b	10.68
urea	0.30	6.10	9.53 (0.08)	10.48 (0.08)	9.81 ^a	10.45 ^a	10.05 ^b	10.28
naphtalene	0.35	5.71	8.10 (0.09)	8.39 (0.09)	8.15 ^c	-	8.25 ^c	8.14
tetracene	0.35	4.89	6.79 (0.08)	6.94 (0.08)	6.84 ^c	-	7.02 ^c	6.97
hexacene	0.35	4.52	6.15 (0.06)	6.33 (0.06)	6.19 ^c	-	6.32 ^c	6.33

^a Ref. 42

^b Ref. 56

^c Ref. 54

Table I. Ionization potentials I for small molecules as calculated by different levels of theory. The G_0W_0 and $\bar{\Delta}GW_0$ estimates were obtained using an LDA starting point and calculated using a stochastic implementation^{45,46} with the statistical errors reported in parentheses. Experimental values are from Ref. 57. For several of the acenes the CCSD(T) results are estimates extrapolated to the infinite basis-set limit.⁵⁴ Molecular geometries were taken from Refs. 57 and 54.

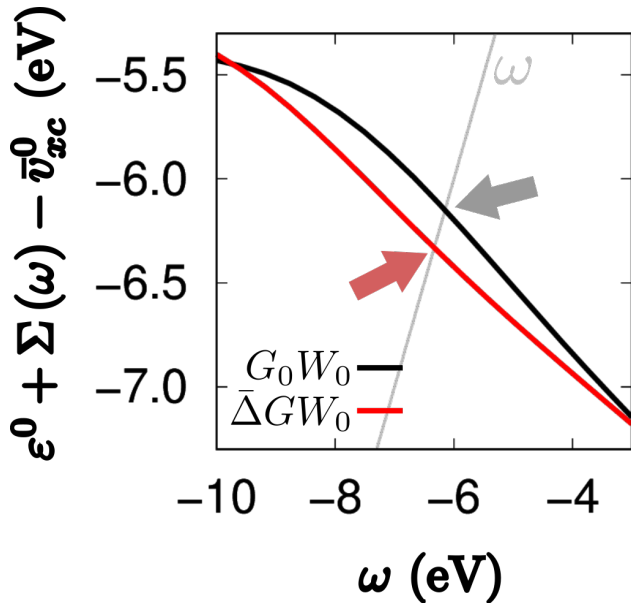


Figure 2. Graphical solution to the QP equation for hexacene for a self-energy from G_0W_0 and $\bar{\Delta}GW_0$. The gray line shows the frequency and the arrows indicate solutions to the fixed point equation (Eq. (3)) and give the QP energy. The $\bar{\Delta}GW$ result is visibly shifted toward a lower energy than the one-shot solution.

and -1.63 ± 0.06 eV for the bottom valence and HOMO states, respectively.

The mean absolute difference between the $\bar{\Delta}GW_0$ and CCSD(T) values is 0.20 eV for molecules, but for the largest systems (tetracene and hexacene) it is only 0.05 eV. This indicates that (i) the scissors operator approximation in Eq. (12) is more appropriate for larger molecules and (ii) $\bar{\Delta}GW_0$ self-consistency is more accurate when G_0W_0 is already a good approximation, i.e., in our case it gives results that are sufficiently close to the CCSD(T) values.

B. Periodic systems

Next we study self-consistency for several periodic solids listed in Table II where we calculate the fundamental band gaps

$$E_g = \varepsilon_L - \varepsilon_H. \quad (15)$$

The stochastic approach is extended here to treat periodic boundary conditions⁵⁸. We again employ LDA with Troullier-Martins pseudopotentials and Fourier real-space grids with a spacing h which is sufficiently small that the eigenvalues are converged to < 10 meV (see Table II). The method is demonstrated on large supercells with 512 atoms (corresponding to $4 \times 4 \times 4$ conventional cells with 2048 valence electrons).

As mentioned earlier, the G_0W_0 treatment of such large systems is enabled by the stochastic approach^{45,46,58}, but our self-consistency scheme is applicable to any G_0W_0 implementation that yields the full-frequency or full-time matrix element of the self-energy.

The results in Table II show that the one-shot correction yields band gaps that are lower than experimental values, in agreement with previous calculations.^{8,20,37,38,43} In all cases studied, self-consistency is quickly achieved within 3 or 4 iterations. The resulting fundamental band gaps are enlarged by as much as 0.20 eV, and are quite close to experiment. The effect of using $\bar{\Delta}GW_0$ on the self-energy curves is illustrated in Fig. 3.

Comparison to previous results (Table II) shows that the $\bar{\Delta}GW_0$ fundamental gaps are overall at least as good as the full eigenvalue self-consistency predictions. In contrast, qp GW band gaps are too high and overestimate experiment by $\sim 10\%$ (also see Ref.⁵⁹).

The $\bar{\Delta}GW_0$ results reproduce well the experimental values, with the exception of bulk silicon. Note, however, that we employ $4 \times 4 \times 4$ conventional cells with Γ point sampling. For silicon, this cell, while very large, is still not large enough to reach the bulk limit. We can still compare our result with the experimental $\Gamma - X$ gap which is higher (1.3 eV⁶⁰). Therefore, overall, for the

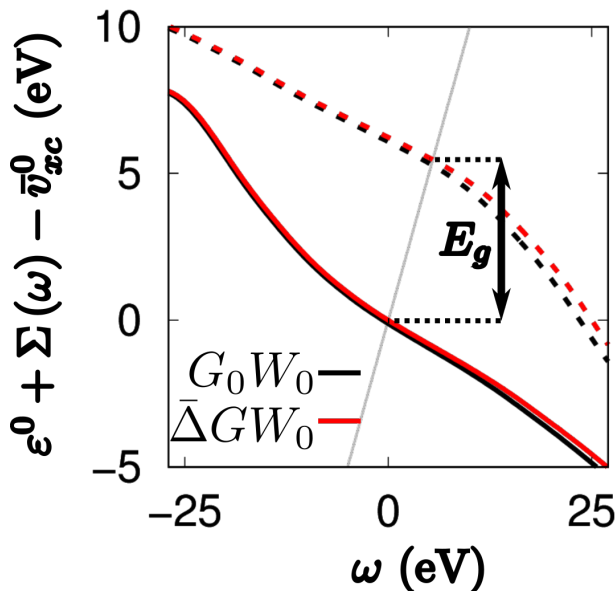


Figure 3. Graphical solution to the QP equation for the G_0W_0 and $\bar{\Delta}GW_0$ self-energies, for a diamond solid simulated by a $4 \times 4 \times 4$ supercell. The gray line denotes the frequency and the intersections with the black and red lines are the solution to the fixed point equation (Eq. (3)). The full and dashed lines are for the top valence and bottom conduction states, respectively. Both axes are shifted so that zero is associated with the QP energy of the top of the valence band as obtained from $\bar{\Delta}GW_0$. The self-consistent result is shifted with a larger band gap (E_g) than the one-shot solution.

set of solids investigated the simplified self-consistency of $\bar{\Delta}GW_0$ yields gaps with excellent mean absolute error of 0.03 eV with respect to experiment.

In all the investigated cases the difference between the QP shifts for the bottom and top valence states are small and correlate slightly with E_g . For BN we observe that in the zeroth iteration (G_0W_0) the bottom valence state and ε_H are shifted by -0.73 ± 0.04 and -0.21 ± 0.03 eV. However, for Si the shifts are 0.13 ± 0.03 and -0.16 ± 0.02 eV.

The excellent performance of $\bar{\Delta}GW$ is surprising but not fortuitous. The structure of the self-energy curve is dominated by plasmon poles^{2,61–63}, and the energy of these poles is proportional to the band gap. The main goal of the iterative treatment is to capture the necessary changes in the plasmon energy. We accomplish this goal by employing a relative shift of occupied vs. unoccupied states that acts like a scissors operator (Eq. (12)) that opens up the band gap and leads to the desired increase in the plasmon frequency.

To test the dependence of the self-energy on energy and its implications for the self-consistency, we further performed a set of complementary calculations for two nanocrystals, $\text{Si}_{35}\text{H}_{36}$ and $\text{Si}_{705}\text{H}_{300}$, studied by stochastic GW in the past^{45,48}. For these crystals we did several calculations at different Kohn-Sham energies at fitted the

QP correction by a quadratic polynomial:

$$\bar{\Delta}(\varepsilon) = a_2(\varepsilon)^2 + a_1\varepsilon + a_0. \quad (16)$$

For the smaller system the QP correction terms are $a_2 = 0.01 \text{ eV}^{-1}$, $a_1 = -0.22$ and $a_0 = -1.13 \text{ eV}$ so $\bar{\Delta}$ is far from being a constant. For the large Si nanocrystal, which is already bulk-like, we find however that $a_2 = 0.00 \text{ eV}^{-1}$, $a_1 = 0.04$ and $a_0 = -1.52 \text{ eV}$, indicating only a weak linear dependence. We conclude that the approximation of rigid shifts of all occupied and all unoccupied states is well justified for solids, for which the variation of the QP shift across the occupied states is much smaller than for molecular systems, making the scissors-like assumption appropriate.

IV. SUMMARY AND CONCLUSIONS

In this paper we derived a general form of Green’s function self-consistency in the time domain and introduced its simplified form, which we label $\bar{\Delta}GW_0$. The underlying assumption of our method is that the differences between Kohn-Sham eigenvalues and quasiparticle energies are approximately just two constants, one for occupied and one for unoccupied states. We approximate this scissors-like correction by the corrections to the HOMO and LUMO energies.

Our approach is merely an *a-posteriori* treatment of the time-dependent self-energy matrix. Hence, $\bar{\Delta}GW_0$ has essentially no additional computational cost beyond that of a one-shot G_0W_0 calculation. In conjunction with the nearly linear scaling stochastic G_0W_0 , it is easily applicable to extremely large systems with thousands of electrons. The combined method is best labeled as stochastic $\bar{\Delta}GW_0$ or just abbreviated as stochastic GW_0 .

We tested stochastic $\bar{\Delta}GW_0$ on molecules and on periodic semiconductors and insulators with large periodic supercells containing 2048 electrons. The predicted ionization potentials and fundamental band gaps are overall much better than one-shot G_0W_0 values when compared to high-level methods and/or experiments. Our simplified self-consistency treatment is especially appropriate for large molecules and periodic systems, and for the latter it yields a mean absolute error of only 0.03 eV.

The stochastic partially self-consistent $\bar{\Delta}GW_0$ approach presented here is both accurate and efficient, opening the door to many future applications in chemistry, physics nano- and material sciences.

ACKNOWLEDGMENTS

V.V., E.R. and D.N. were supported by the Center for Computational Study of Excited State Phenomena in Energy Materials (C2SEPEM) at the Lawrence Berkeley National Laboratory, which is funded by the U.S. Department of Energy, Office of Science, Basic Energy Sciences, Materials Sciences and Engineering Division under

system	h (a_0)	E_g (eV)					
		LDA	G_0W_0	ΔGW_0	evGW (Ref. 43)	qpGW (Ref. 43)	Exp.
Si	0.446	0.56	1.29 (0.04)	1.35 (0.04)	1.20*	1.28*	1.3 ^a (1.17*) ^a
SiC	0.293	1.37	2.29 (0.04)	2.35 (0.04)	2.43	2.64	2.42 ^b
AlP	0.368	1.46	2.41 (0.03)	2.50 (0.03)	2.59	2.77	2.52 ^c
C	0.336	4.16	5.40 (0.06)	5.47 (0.06)	5.50	5.99	5.48 ^d
BN	0.380	4.48	6.21 (0.06)	6.41 (0.07)	6.10	6.73	6.1 - 6.4 ^e

^a Ref. 60

^b Ref. 64

Table II. Fundamental band gaps (E_g) for a sample of solids. For each system a $4 \times 4 \times 4$ conventional super-cell (with 2048 valence electrons) was used. Values labeled by * are for the minimum fundamental gap, which is not accessed in our calculations (see text).

contract No. DEAC02-05CH11231 as part of the Computational Materials Sciences Program. R.B. is grateful for support by the Binational Science Foundation, Grant 2015687 and for support from the Israel Science Founda-

tion – FIRST Program, Grant No. 1700/14. The calculations were performed as part of the XSEDE computational Project No. TG-CHE170058⁶⁵.

* vojtech.vlcek@gmail.com

† roi.baer@huji.ac.il

‡ eran.rabani@berkeley.edu

§ dxn@ucla.edu

¹ L. Hedin, Phys. Rev. **139**, A796 (1965).

² F. Aryasetiawan and O. Gunnarsson, Rep. Prog. Phys. **61**, 237 (1998).

³ M. M. Rieger, L. Steinbeck, I. White, H. Rojas, and R. Godby, Comput. Phys. Commun. **117**, 211 (1999).

⁴ L. Steinbeck, A. Rubio, L. Reining, M. Torrent, I. White, and R. Godby, Comput. Phys. Commun. **125**, 05 (1999).

⁵ G. Onida, L. Reining, and A. Rubio, Rev. Mod. Phys. **74**, 601 (2002).

⁶ A. Rubio and S. G. Louie, “Quasiparticle AND optical properties of solids AND nanostructures: The gw-bse approach,” in *Handbook of materials modeling*, edited by S. Yip (Springer, Dordrecht ; New York, 2005) p. 215.

⁷ C. Friedrich and A. Schindlmayr, NIC Series **31**, 335 (2006).

⁸ M. Shishkin and G. Kresse, Phys. Rev. B **75**, 235102 (2007).

⁹ P. E. Trevisanutto, C. Giorgetti, L. Reining, M. Ladisa, and V. Olevano, Phys. Rev. Lett. **101**, 226405 (2008).

¹⁰ C. Rostgaard, K. W. Jacobsen, and K. S. Thygesen, Phys. Rev. B **81**, 085103 (2010).

¹¹ I. Tamblyn, P. Darancet, S. Y. Quek, S. A. Bonev, and J. B. Neaton, Phys. Rev. B **84**, 201402 (2011).

¹² M. van Setten, F. Weigend, and F. Evers, J. Chem. Theory Comput. **9**, 232 (2012).

¹³ G. Stefanucci and R. van Leeuwen, *Nonequilibrium Many-Body Theory of Quantum Systems: A Modern Introduction* (Cambridge University Press, 2013).

¹⁴ M. Govoni and G. Galli, J. Chem. Theory Comput. **11**, 2680 (2015).

¹⁵ F. Kaplan, M. E. Harding, C. Seiler, F. Weigend, F. Evers, and M. J. van Setten, J. Chem. Theory Comput. (2016).

¹⁶ M. S. Hybertsen and S. G. Louie, Phys. Rev. Lett. **55**, 1418 (1985).

¹⁷ M. S. Hybertsen and S. G. Louie, Phys. Rev. B **34**, 5390

(1986).

¹⁸ W. Kohn and L. J. Sham, Phys. Rev. **140**, A1133 (1965).

¹⁹ P. Hohenberg and W. Kohn, Phys. Rev. **136**, B864 (1964).

²⁰ S. V. Faleev, M. van Schilfgaarde, and T. Kotani, Phys. Rev. Lett. **93**, 126406 (2004).

²¹ F. Caruso, P. Rinke, X. Ren, M. Scheffler, and A. Rubio, Phys. Rev. B **86**, 081102 (2012).

²² F. Bruneval and M. A. Marques, J. Chem. Theory Comput. **9**, 324 (2012).

²³ F. Bruneval, J. Chem. Phys. **136**, 194107 (2012).

²⁴ M. J. van Setten, F. Caruso, S. Sharifzadeh, X. Ren, M. Scheffler, F. Liu, J. Lischner, L. Lin, J. R. Deslippe, S. G. Louie, C. Yang, F. Weigend, J. B. Neaton, F. Evers, and P. Rinke, J. Chem. Theory Comput. **11**, 5665 (2015).

²⁵ J. W. Knight, X. Wang, L. Gallandi, O. Dolgounitcheva, X. Ren, J. V. Ortiz, P. Rinke, T. Körzdörfer, and N. Marom, J. Chem. Theory Comput. (2016).

²⁶ A. Stan, N. E. Dahlen, and R. van Leeuwen, Europhysics Lett. **76**, 298 (2006).

²⁷ A. Stan, N. E. Dahlen, and R. van Leeuwen, J. Chem. Phys. **130**, 114105 (2009).

²⁸ C. Rostgaard, K. W. Jacobsen, and K. S. Thygesen, Phys. Rev. B **81**, 085103 (2010).

²⁹ X. Blase and C. Attaccalite, Appl. Phys. Lett. **99**, 171909 (2011).

³⁰ J. Deslippe, G. Samsonidze, D. A. Strubbe, M. Jain, M. L. Cohen, and S. G. Louie, Comput. Phys. Commun. **183**, 1269 (2012).

³¹ H.-V. Nguyen, T. A. Pham, D. Rocca, and G. Galli, Phys. Rev. B **85**, 081101 (2012).

³² F. Caruso, P. Rinke, X. Ren, M. Scheffler, and A. Rubio, Phys. Rev. B **86**, 081102 (2012).

³³ F. Caruso, P. Rinke, X. Ren, A. Rubio, and M. Scheffler, Phys. Rev. B **88**, 075105 (2013).

³⁴ P. Koval, D. Foerster, and D. Sánchez-Portal, Phys. Rev. B **89**, 155417 (2014).

³⁵ L.-W. Wang, Phys. Rev. B **91**, 125135 (2015).

³⁶ B. Holm and U. von Barth, Phys. Rev. B **57**, 2108 (1998).

³⁷ F. Bruneval and M. Gatti, in *First Principles Ap-*

- proaches to Spectroscopic Properties of Complex Materials* (Springer, 2014) pp. 99–135.
- ³⁸ M. van Schilfgaarde, T. Kotani, and S. Faleev, *Phys. Rev. Lett.* **96**, 226402 (2006).
- ³⁹ T. Kotani, M. van Schilfgaarde, and S. V. Faleev, *Phys. Rev. B* **76**, 165106 (2007).
- ⁴⁰ F. Kaplan, F. Weigend, F. Evers, and M. van Setten, *J. Chem. Theory Comput.* **11**, 5152 (2015).
- ⁴¹ F. Kaplan, M. Harding, C. Seiler, F. Weigend, F. Evers, and M. van Setten, *J. Chem. Theory Comput.* **12**, 2528 (2016).
- ⁴² F. Caruso, M. Dauth, M. J. van Setten, and P. Rinke, *J. Chem. Theory Comput.* **12**, 5076 (2016).
- ⁴³ M. Shishkin and G. Kresse, *Phys. Rev. B* **75**, 235102 (2007).
- ⁴⁴ J. E. Northrup, M. S. Hybertsen, and S. G. Louie, *Phys. Rev. Lett.* **59**, 819 (1987).
- ⁴⁵ D. Neuhauser, Y. Gao, C. Arntsen, C. Karshenas, E. Rabani, and R. Baer, *Phys. Rev. Lett.* **113**, 076402 (2014).
- ⁴⁶ V. Vlček, E. Rabani, D. Neuhauser, and R. Baer, *J. Chem. Theory Comput.* **13**, 4997 (2017).
- ⁴⁷ V. Vlček, H. R. Eisenberg, G. Steinle-Neumann, D. Neuhauser, E. Rabani, and R. Baer, *Phys. Rev. Lett.* **116**, 186401 (2016).
- ⁴⁸ V. Vlček, E. Rabani, and D. Neuhauser, *Phys. Rev. Mater.* **2**, 030801 (2018).
- ⁴⁹ M. R. Filip and F. Giustino, *Phys. Rev. B* **90**, 245145 (2014).
- ⁵⁰ X. Qian, P. Umari, and N. Marzari, *Phys. Rev. B* **91**, 245105 (2015).
- ⁵¹ G. J. Martyna and M. E. Tuckerman, *J. Chem. Phys.* **110**, 2810 (1999).
- ⁵² J. P. Perdew and Y. Wang, *Phys. Rev. B* **45**, 13244 (1992).
- ⁵³ N. Troullier and J. L. Martins, *Phys. Rev. B* **43**, 1993 (1991).
- ⁵⁴ T. Rangel, S. M. Hamed, F. Bruneval, and J. B. Neaton, *J. Chem. Theory Comput.* **12**, 2834 (2016).
- ⁵⁵ M. J. van Setten, F. Caruso, S. Sharifzadeh, X. Ren, M. Scheffler, F. Liu, J. Lischner, L. Lin, J. R. Deslippe, S. G. Louie, *et al.*, *J. Chem. Theory Comput.* **11**, 5665 (2015).
- ⁵⁶ K. Krause, M. E. Harding, and W. Klopper, *Mol. Phys.* **113**, 1952 (2015).
- ⁵⁷ “Nist computational chemistry comparison and benchmark database nist standard reference database, number 101; johnson, r. d., iii, ed.; 2016. <http://cccbdb.nist.gov/>,”.
- ⁵⁸ V. Vlček, E. Rabani, and D. Neuhauser, to be submitted (2018).
- ⁵⁹ K. van Houcke, I. S. Tupitsyn, A. S. Mishchenko, and N. V. Prokof’ev, *Phys. Rev. B* **95**, 195131 (2017).
- ⁶⁰ M. L. Tiago, S. Ismail-Beigi, and S. G. Louie, *Phys. Rev. B* **69**, 125212 (2004).
- ⁶¹ M. S. Hybertsen and S. G. Louie, *Phys. Rev. B* **34**, 5390 (1986).
- ⁶² R. W. Godby and R. J. Needs, *Phys. Rev. Lett.* **62**, 1169 (1989).
- ⁶³ P. Larson, M. Dvorak, and Z. Wu, *Phys. Rev. B* **88**, 125205 (2013).
- ⁶⁴ D. Bimberg, M. Altarelli, and N. Lipari, *Solid State Comm.* **40**, 437 (1981).
- ⁶⁵ J. Towns, T. Cockerill, M. Dahan, I. Foster, K. Gaither, A. Grimshaw, V. Hazlewood, S. Lathrop, D. Lifka, G. D. Peterson, *et al.*, *Computing in Science & Engineering* **16**, 62 (2014).